

# MONTE CARLO GAMMA TRANSMISSION MODEL FOR CHARACTERIZATION OF MULTI-GAMMA SHIELDING PARAMETERS OF SOME HEAVY METAL OXIDE GLASSES

by

*Nassreldeen A. A. ELSHEIKH*

Department of Physics, College of Science & Arts, Al-Baha University, Al-Mikhwah, Al-Baha, Saudi Arabia

Scientific paper

<https://doi.org/10.2298/NTRP2104338E>

The applicability of a simple Monte Carlo gamma transmission model was investigated by characterizing the mass attenuation coefficient, mean free path, and half-value layer for six glass sample simulants of the  $\text{PbO-Li}_2\text{O-B}_2\text{O}_3$  system previously prepared by others. The mass attenuation coefficients were calculated and compared with those of XCOM and the available experimental data for twenty gamma energy lines from 0.107 MeV to 7.12 MeV, and good agreement was obtained. The effects of PbO concentration on the simulated values of mass attenuation coefficient, mean free path, and half-value layer, were calculated and compared with available experimental data in the gamma energy range 0.356-1.332 MeV, and good agreement was found. The glass sample with the optimal gamma shielding for all considered gamma energies was the sample with the chemical formula  $\text{Pb}_3\text{B}_4\text{O}_9$ . On the one hand, the Monte Carlo results confirm the applicability of the proposed model for performing additional calculations of photon attenuation properties for different glass compositions, and on the other hand, considering the energy range of gamma-ray photons in a reactor during uranium fission, 0.10-10 MeV, the results suggest the use of the studied glass samples as optical shielding windows in nuclear reactors.

*Key words: Monte Carlo simulation, XCOM, heavy metal oxide glass, gamma shielding parameter*

## INTRODUCTION

The computing and measuring of gamma-ray shielding parameters such as mass attenuation coefficient,  $\mu/\rho$ , [ $\text{cm}^2\text{g}^{-1}$ ], half-value layer (HVL) in cm, and mean free path (MFP) in cm play an important role in the research area of radiation physics [1]. The mass attenuation coefficient is the most commonly used parameter to study the interaction of gamma radiation [2-6]. This interaction is a combination of partial photoelectric absorption, Compton scattering, and pair production, which depend on the energy and atomic number. Photoelectric absorption and pair production are the processes by which the photon is completely removed, while the Compton interaction slows down the photon energy sufficiently to be removed by the photoelectric absorption interaction [4]. Thus,  $\mu/\rho$  is the most important quantity characterizing the shielding design and is a fundamental factor for deriving other gamma-ray shielding parameters such as MFP and HVL.

Concrete is commonly used as a shielding material in nuclear reactors for various types of nuclear radiation [1, 7-8]. However, concrete as a shielding ma-

terial in nuclear reactors is subject to several limitations. These include the constant change in the shielding properties due to the addition of moisture content, opacity to visible light so that it is not possible to see through the concrete shielding, cracking after long exposure to nuclear radiation and aging, and water loss in the concrete shielding due to heat generated in the concrete by nuclear radiation [1, 9].

Various configurations of heavy metal oxide glass systems have been investigated as possible alternatives to concrete for gamma-ray shielding, and several geometries for gamma transmission have been developed [4, 10-14]. Heavy metal oxide glasses are transparent to visible light and their chemical composition can be varied over wide ranges to attenuate different types of nuclear radiation generated in nuclear reactors [1]. The transparent property of heavy metal oxide glasses makes them useful for optical windows in nuclear reactors and isotope technology centers.

In light of these efforts, Kumar [15] measured the  $\mu/\rho$  values for six glass samples of composition (0.6-x)  $\text{PbO-x Li}_2\text{O-0.40 B}_2\text{O}_3$  (where  $0 < x < 0.25$  mol%) at photon energies; 0.356, 0.662, 1.173, and 1.332 MeV in a narrow beam geometrical set-up consisting of a 4.5 cm  $\times$  5.1 cm NaI(Tl) detector with an

\* Author s e-mail: [nassreldeen.elsheikh@yahoo.com](mailto:nassreldeen.elsheikh@yahoo.com)

energy resolution of 12.5 % at 0.662 MeV located at 66 cm from the gamma-ray source.

Three lead collimators were used: two of them to direct the initial gamma-rays from the source to the glass sample and the other to collimate the transmitted photons toward the NaI detector. The gamma-ray source, NaI detector, and lead collimators were housed in a lead shielding container.

The measured  $\mu/\rho$  values were then used to obtain the MFP, effective atomic number, and electron density values. The shielding capabilities of the prepared glasses were also compared with standard concretes as well as with the standard shielding glasses. It was found that the prepared glasses are the better shielding alternative to the conventional concretes as well as to other standard shielding glasses, with the most effective shielding properties observed for the sample with the chemical formula  $Pb_3B_4O_9$ .

The lead shielding container can reduce the background gamma photons measured by the NaI detector. However, it increases the system geometry and affects the readout of the NaI detector. In addition, the use of multiple lead collimators can present geometric challenges in terms of configuration and adjustment. In addition, the relatively large distance (66 cm) between the source and detector may affect the efficiency of the NaI detector [16].

On the other hand, the four energy lines used in [15], 0.356, 0.662, 1.173, and 1.332 MeV, do not represent all the expected gamma-ray energies that could be used to examine the gamma-shielding capabilities of the prepared glass samples. Moreover, it was found that the energy range of gamma-ray photons in a reactor during uranium fission is 0.10-10 MeV [3]. Therefore, for a possible application of such glasses as transparent windows in nuclear reactors, it is essential to have  $\mu/\rho$  values for a wider range of photon energies. On the other hand, HVL is one of the fundamental parameters for gamma-ray shielding that could be used to determine the design of the shielding, but it is missing in [15]. This work addresses these shortcomings by modeling a simpler Monte Carlo (MC) model for gamma transmission and examining the shielding performance of the six glass samples used in [15] at gamma energy lines of a wider range.

The MCNP radiation transport code [17] can, in principle, provide the highest accuracy and precision in modeling the physical interactions in a matter applied in circumstances often unavailable for experimental measurements. From the literature [2, 4, 18-21], MCNP is an effective tool for simulating gamma transmission geometries and calculating  $\mu/\rho$  values for different types of compounds or mixtures.

On the other hand, the computer program XCOM [22] is usually used for the theoretical estimation of  $\mu/\rho$  values and interaction cross sections for elements, compounds, and mixtures. The XCOM program calculates the  $\mu/\rho$  values in the gamma energy

range 1 keV-100 GeV using the Hartree-Slater central potential theory and it has been experimentally verified to give results that are close to the experimental results [23, 24].

Based on such considerations, MCNP5 [17] was used to model a simple gamma transmission geometry suitable for exploring the gamma shielding properties of the six glass sample simulants of the  $PbO-Li_2O-B_2O_3$  system previously prepared by Kumar [15]. To evaluate the suitability of the glass samples as optical shielding windows in nuclear reactors, the geometrical model was used to determine the  $\mu/\rho$  values at twenty gamma energy lines: 0.107, 0.114, 0.122, 0.139, 0.159, 0.170, 0.182, 0.208, 0.238, 0.254, 0.271, 0.276, 0.356, 0.511, 0.662, 0.835, 1.173, 1.275, 1.332 and 7.12 MeV. These energies cover a reasonable range to study the gamma-shielding capabilities of the simulated glass samples and correspond to the energy range of gamma-rays occurring in nuclear reactors during uranium fission [3]. In addition, the XCOM program was used to calculate the  $\mu/\rho$  values for the same gamma energy lines, and the results were compared with those of MCNP. This serves to improve the accuracy of the simulated MCNP values and to evaluate the applicability of the proposed geometry for gamma transmission predictions.

The experimental values of MFP reported in [15] were used to derive the HVL values for the six glass samples. The values of  $\mu/\rho$ , MFP, and HVL, as well as the experimental results for the effect of PbO concentration on these gamma-shielding parameters [15], were compared with the MCNP values at gamma energy lines; 0.356, 0.662, 1.173, and 1.332 MeV.

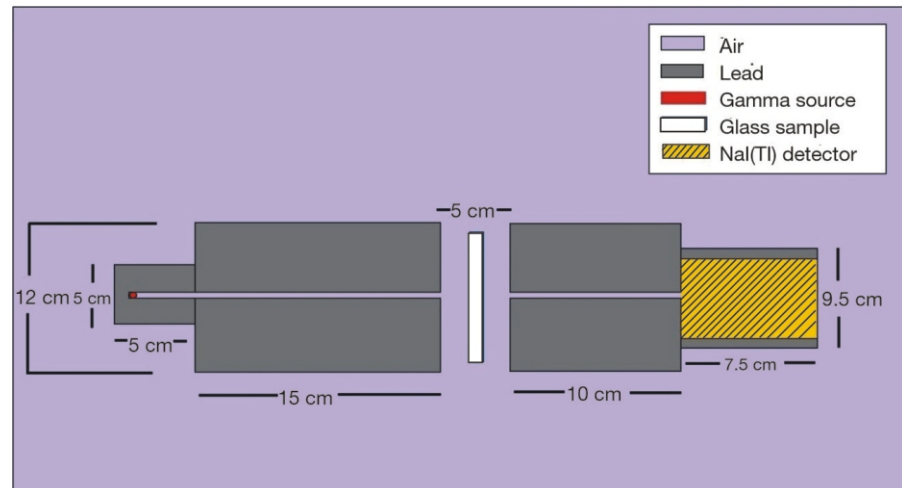
## MATERIALS AND METHODS

Appropriate geometry and input data for the proposed gamma transmission model were modeled to reduce the potential statistical and systematic errors that could affect the precision and accuracy of the MCNP values. The simulated MCNP geometry is shown in fig. 1. The model consists of a cylindrical lead, Pb, capsule with an inner diameter of 1 cm, an outer diameter of 5 cm, a length of 4 cm for the cavity, and a length of 5 cm for the Pb capsule. The Pb capsule contains the gamma source, which is considered to be a mono-energetic isotropic point source in an infinite medium.

The original direction of the gamma source was parallel to the beam axis, which was assumed to be the X-axis. The source strength was set to unity to represent a normalized source, and the MCNP code was executed in photon transport mode only. The photon weighting factor is 1 in all cells and zero in the cutoff region (outside the boundary surface of the problem). The cross-sections were taken from the ENDF/B-VI and the NJOY libraries.

The initial gamma-rays from the source were collimated by a cylindrical lead collimator of 1 cm inner diameter, 12 cm outer diameter, and 15 cm length. The

**Figure 1. Geometrical model employed for the MCNP simulations**



thicknesses of the glass samples in [15] range from 0.684 cm to 0.741 cm. However, the glass sample in this work was simulated as a cylindrical disc with 10 cm diameter and 0.7 cm thickness. The transmitted photons were collimated by a cylindrical lead collimator with 1 cm inner diameter, 12 cm outer diameter, and 10 cm length. It is worth noting that the glass sample was 2.5 cm along the X-axis from the two collimators of the gamma source and the transmitted photons.

To count the intensity ( $I$ ) of transmitted photons, a 7.5 cm  $\times$  7.5 cm NaI (Tl) detector was modeled and partially shielded (considering the readout of a physical NaI detector) with a cylindrical Pb collimator of 1 cm thickness. Pulse height tally F8 was selected to calculate the energy deposition in the NaI(Tl) detector, with the direction of photons being normal to the surface of the detector. To increase the precision of the results, the statistical error was reduced by performing the MCNP calculations with  $10^7$  histories and counting the transmitted spectrum for 100 seconds. These options provided a sufficient number of counts (fraction of histories that hit the NaI detector), resulting in a statistical error of less than 0.3 %.

The accuracy of the MCNP results was increased by broadening the initial responses of the NaI detector using the Gaussian energy broadening option (GEB) [17]. The GEB is a special treatment for the detector response called by inserting the FTn option into the tally card of the MCNP input file. This is intended to better simulate a physical radiation detector in which the energy peaks exhibit Gaussian energy broadening, thus reducing the effects of such systematic error.

The energy resolution [%] of the detector was defined by the full width at half maximum (FWHM), of a single photopeak using the following eqs. [25, 26]

$$R = \frac{FWHM}{E_0} \times 100 [\%] \quad (1)$$

$$FWHM = 2\sqrt{2 \ln 2} \sigma \quad (2)$$

Here  $R$  is the energy resolution,  $E_0$  – the central energy of the photopeak, and  $\sigma = \sqrt{\bar{N}}$  – the standard deviation for the mean number of counts  $\bar{N}$  generated in the NaI detector.

The use of the XCOM software requires knowledge of the mass fractions of each constituent for each glass sample. Therefore, the mole fractions of PbO, Li<sub>2</sub>O, and B<sub>2</sub>O<sub>3</sub> were converted to mass fractions for each glass sample using the formula

$$\chi_i = \frac{n_i M_i}{\sum_{i=1}^N n_i M_i} \quad (3)$$

where  $\chi_i$  [g] is the mass fraction of one constituent compound. The term  $n_i M_i$  – the mass [g] of the constituent compound, consisting of its mole fraction  $n_i$  [mol] and its molar mass [g mol<sup>-1</sup>]. While the term  $\sum_{i=1}^N n_i M_i$  represents the total mass [g] of the mixture.

The mass fractions of the constituents of each glass sample were inserted in the XCOM database program to determine the theoretical  $\mu/\rho$  values at gamma energy lines from 0.107 to 7.12 MeV. It is worth noting that the XCOM software generates not only the  $\mu/\rho$  values but also the elemental mass fractions for each glass sample. These elemental mass fractions are needed to specify the materials of the glass samples (by a mass fraction) in the MCNP input files. Therefore, the MCNP simulations for each glass sample were performed using the XCOM analysis results in terms of the elemental mass fractions of each sample.

The linear attenuation coefficient  $\mu$  [cm<sup>-1</sup>] of the studied glass samples is defined from the exponential attenuation rule for narrow monochromatic beams for thin absorbing material [27]

$$I = I_0 e^{-\mu t} \quad (4)$$

The total values of the  $\mu/\rho$  [cm<sup>2</sup>g<sup>-1</sup>] for materials with multiple elements are the sum of the  $(\mu/\rho)_i$  values of the individual elements using mixture rule [28]

$$\mu/\rho = \sum_i w_i (\mu/\rho)_i \quad (5)$$

where  $w_i$  is the weight fraction and  $(\mu/\rho)_i$  – the mass attenuation coefficient of the  $i$ th constituent element.

The values of  $\mu$  were used to determine MFP and HVL for each glass sample. The MFP [cm] is the thickness of the shielding materials for two successive collisions and was calculated in [3] as follows

$$\text{MFP} = \frac{1}{\mu} \quad (6)$$

The HVL [cm], is the thickness of the shielding materials that reduce the photon density by 50 % of the incident radiation. The HVL is expressed in units of length [29]

$$\text{HVL} = \frac{0.693}{\mu} \quad (7)$$

Based on eq. (7), the experimental values of HVL to be compared with those obtained by MCNP simulations were derived by multiplying the measured values of MFP for the six prepared glass samples by  $\ln(2) \cdot 0.693$ .

The simulated glass samples were targeted using the spectra of gamma-ray photons from the point

source, while the intensities of the transmitted photons for gamma energy lines; 0.107, 0.114, 0.122, 0.139, 0.159, 0.170, 0.182, 0.208, 0.238, 0.254, 0.271, 0.276, 0.356, 0.511, 0.662, 0.835, 1.173, 1.275, 1.332, and 7.12 MeV were calculated. The transmitted intensity,  $I$ , and initial intensity,  $I_0$ , of the photons were calculated with and without the glass sample, respectively. For each glass sample, the linear attenuation coefficients  $\mu$  [ $\text{cm}^{-1}$ ] were determined using eq. (4) and then used to determine the  $\mu/\rho$  values. The mole fractions, chemical formulas, densities, and thicknesses of the glass samples studied are listed in tab. 1 [15].

## RESULTS AND DISCUSSION

The MCNP values of  $\mu/\rho$  for the six simulated glass samples were compared with those calculated theoretically by XCOM and with the available experimental results reported by Kumar in [15]. The data were organized and presented in tab. 2. From tab. 2, it can be seen that  $\mu/\rho$  of each glass sample decreases sharply in

**Table 1. The mole fractions, chemical formulas, densities, and thicknesses of the investigated glass samples [15]**

Sample	Mole fractions			Chemical formula	Density [ $\text{gcm}^{-3}$ ]	Thickness [cm]
	PbO	Li <sub>2</sub> O	B <sub>2</sub> O <sub>3</sub>			
Sample 1	0.60	0.00	0.40	Pb <sub>3</sub> B <sub>4</sub> O <sub>9</sub>	6.306	0.741
Sample 2	0.55	0.05	0.40	Pb <sub>11</sub> B <sub>16</sub> Li <sub>2</sub> O <sub>36</sub>	6.144	0.712
Sample 3	0.50	0.10	0.40	Pb <sub>3</sub> B <sub>8</sub> Li <sub>2</sub> O <sub>18</sub>	5.786	0.648
Sample 4	0.45	0.15	0.40	Pb <sub>9</sub> B <sub>16</sub> Li <sub>6</sub> O <sub>36</sub>	5.553	0.659
Sample 5	0.40	0.20	0.40	Pb <sub>2</sub> B <sub>4</sub> Li <sub>2</sub> O <sub>9</sub>	5.378	0.756
Sample 6	0.35	0.25	0.40	Pb <sub>7</sub> B <sub>16</sub> Li <sub>10</sub> O <sub>36</sub>	5.138	0.684

**Table 2. The MCNP, XCOM, and available experimental data [15] of  $\mu/\rho$  for the six glass samples at gamma energy lines from 0.107 MeV to 7.12 MeV**

Energy (MeV)	Mass attenuation coefficients [ $\text{cm}^2\text{g}^{-1}$ ]																	
	Sample 1			Sample 2			Sample 3			Sample 4			Sample 5			Sample 6		
	MCNP	XCOM	Exp.*	MCNP	XCOM	Exp.	MCNP	XCOM	Exp.	MCNP	XCOM	Exp.	MCNP	XCOM	Exp.	MCNP	XCOM	Exp.
0.107	3.7151	3.6630		3.6251	3.5750		3.5241	3.4740		3.4251	3.3600		3.2921	3.2270		3.1361	3.0710	
0.114	3.1056	3.0990		3.1016	3.0250		2.9476	2.9400		2.8516	2.8440		2.7466	2.7320		2.6165	2.6020	
0.122	2.6705	2.6250		2.6085	2.5630		2.5376	2.4920		2.4366	2.4110		2.3426	2.3170		2.2336	2.2070	
0.139	1.9016	1.8910		1.8576	1.8470		1.8076	1.7970		1.7506	1.7400		1.6836	1.6730		1.6064	1.5960	
0.159	1.3847	1.3690		1.3437	1.3380		1.3157	1.3020		1.2747	1.2620		1.2277	1.2150		1.1725	1.1600	
0.170	1.1774	1.1650		1.1514	1.1390		1.1214	1.1090		1.0874	1.0760		1.0474	1.0360		1.0017	0.9903	
0.182	1.0198	0.9931		0.9880	0.9713		0.9732	0.9465		0.9449	0.9181		0.9120	0.8852		0.8735	0.8467	
0.208	0.7495	0.7287		0.7411	0.7133		0.7167	0.6959		0.6968	0.6760		0.6737	0.6529		0.6466	0.6258	
0.238	0.5542	0.5410		0.5455	0.5303		0.5312	0.5180		0.5232	0.5040		0.5070	0.4878		0.4881	0.4689	
0.254	0.4738	0.4689		0.4658	0.4599		0.4545	0.4496		0.4428	0.4379		0.4342	0.4243		0.4183	0.4084	
0.271	0.4148	0.4082		0.4132	0.4006		0.4009	0.3920		0.3911	0.3822		0.3807	0.3708		0.3674	0.3575	
0.276	0.4148	0.4082		0.4132	0.4006		0.4009	0.3920		0.3911	0.3822		0.3807	0.3708		0.3674	0.3575	
0.356	0.2501	0.2436	0.240	0.2456	0.2399	0.235	0.2406	0.2357	0.233	0.2349	0.2309	0.228	0.2285	0.2253	0.220	0.2213	0.2188	0.215
0.511	0.1451	0.1397		0.1432	0.1383		0.1411	0.1367		0.1387	0.1348		0.1361	0.1327		0.1331	0.1302	
0.662	0.1045	0.1022	0.101	0.1042	0.1015	0.100	0.1028	0.1007	0.0995	0.1015	0.0998	0.0985	0.1000	0.0987	0.0971	0.0986	0.0975	0.0968
0.835	0.0828	0.0810		0.0821	0.0806		0.0814	0.0802		0.0806	0.0797		0.0798	0.0792		0.0790	0.0786	
1.173	0.0611	0.0608	0.0601	0.0609	0.0607	0.0598	0.0608	0.0606	0.0598	0.0607	0.0605	0.0594	0.0605	0.0603	0.0591	0.0603	0.0601	0.0589
1.275	0.0581	0.0573		0.0579	0.0573		0.0576	0.0572		0.0573	0.0571		0.0570	0.0569		0.0569	0.0568	
1.332	0.0563	0.0557	0.0551	0.0560	0.0556	0.0549	0.0558	0.0556	0.0548	0.0556	0.0555	0.0546	0.0555	0.0554	0.0542	0.0553	0.0552	0.0539
7.120	0.0433	0.0403		0.0426	0.0398		0.0419	0.0393		0.0411	0.0387		0.0402	0.0380		0.0392	0.0372	

\*Exp. – experiment

the low energy region 0.107-0.356 MeV. This can be attributed to the photoelectric effect that prevails at  $E < 0.4$  MeV [30]. The  $\mu/\rho$  values then gradually decrease in the higher energy region 0.356-7.12 MeV for all glass samples considered. This can be attributed to the fact that Compton scattering and pair production are the predominant responses in the  $0.4 \text{ MeV} < E < 1.330$  MeV and  $E > 1.02$  ranges [29, 30].

As a measure of agreement, the percent relative differences RD(%) between (MCNP and XCOM) at gamma energy lines from 0.107 to 7.12 MeV and (MCNP and experiment) at gamma energy lines; 0.356, 0.662, 1.173, and 1.332 MeV, were calculated for all glass samples considered with respect to the  $\mu/\rho$  values. The average of the RD [%] values for each glass sample was calculated and the results are presented in tab. 3. As can be seen in tab. 3, the averaged RD between (MCNP and XCOM) and (MCNP and Experiment)  $\mu/\rho$  values are very small and are in the ranges 1.93-1.77 % and 2.79-2.38 %, respectively. Therefore, a satisfactory agreement is achieved and it can be concluded that the proposed gamma transmission geometry is suitable for estimating the  $\mu/\rho$  values for the six glass samples at the gamma energy lines under investigation.

The discrepancies between the MCNP and experimental values of  $\mu/\rho$  could be attributed to several sources of systematic error. The simplification of the geometric model of the MCNP, fig. 1, is one of these sources. The distance between the source and the detector was reduced to 35 cm to improve the efficiency of the NaI detector [16], and the lead shielding container as well as the three lead collimators used in [15] were eliminated. On the other hand, the discrepancies could be due to the uncertainty in the energy resolution of the NaI(Tl) detector model. Also, the uncertainties in the cross-section data libraries and the material composition in the current MCNP simulations could be additional sources of systematic errors that affect the accuracy of the current MCNP simulations.

The differences in the MCNP and XCOM values can be attributed to the differences in the cross-section data libraries considered for each method and the different nature of the two techniques used. The MCNP code models the physical interactions in a matter, whereas

**Table 3. Average of relative differences RD [%] between (MCNP and XCOM) and (MCNP and experiment) values of  $\mu/\rho$**

Sample	RD [%] (MCNP-XCOM)	RD [%] (MCNP-Exp.*)
Sample 1	1.9306	2.7889
Sample 2	2.1037	3.0293
Sample 3	1.8059	2.4514
Sample 4	1.7510	2.4583
Sample 5	1.7879	2.8191
Sample 6	1.7684	2.3814

\*Exp. – experiment

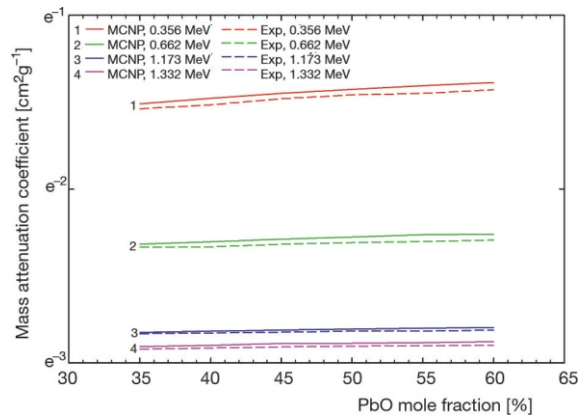


**Figure 2. Variation of MCNP and measured [15]  $\mu/\rho$  values with PbO concentration at gamma energy range 0.356-1.332 MeV**

the XCOM computer program is typically used for theoretical estimates. In addition, the differences could be due to the statistical uncertainties in the MCNP results, which were reported to be less than 0.3 %.

The effect of PbO concentration (mole fraction %) on the  $\mu/\rho$  parameter was also investigated. Figure 2 shows the variation of the simulated and experimentally measured  $\mu/\rho$  values with the PbO contribution at the four gamma energy lines: 0.356, 0.662, 1.173, and 1.332 MeV. As can be seen in fig. 2, both the simulated and measured  $\mu/\rho$  values increase with increasing PbO concentration and decrease with increasing photon energy, with the best gamma shielding for the sample with the chemical formula  $\text{Pb}_3\text{B}_4\text{O}_9$  with 60 % PbO at 0.356 MeV. The results regarding the variation of simulated  $\mu/\rho$  values with incident photon energy, listed in tab. 2, and with PbO concentration, presented in fig. 2, are in agreement with those of Kumar [15].

The results related to the variation of the simulated and measured  $\mu/\rho$  values with the energy of the incident photons as well as with the PbO concentration imply that if we increase the energy of the incident photons, we will obtain lower  $\mu/\rho$  values and therefore higher MFP and HVL values. On the other hand, if we increase the PbO concentration, we will obtain higher  $\mu/\rho$  values and thus lower MFP and HVL values. To investigate this conclusion, the simulated values of MFP and HVL were compared with the experimentally measured values for the six glass simulants at gamma energy lines of 0.356, 0.662, 1.173, and 1.332 MeV. The results are presented in tabs. 4 and 5, respectively. In addition, the variations of simulated and measured MFP and HVL values with PbO concentration at gamma energy lines of 0.356, 0.662, 1.1732, and 1.332 MeV were graphically shown in figs. 3 and 4, respectively. As expected, tabs. 4 and 5 and figs. 3 and 4 show that both MFP and HVL values increase with the increase of photon energies and decrease with the increase of PbO concentration, for all six simulated glass samples.

**Table 4. The MCNP and available experimental data [15] of MFP for the six glass samples at gamma energy range (0.356-1.332) MeV**

Energy [MeV]	MFP [cm]											
	Sample 1		Sample 2		Sample 3		Sample 4		Sample 5		Sample 6	
	MCNP	Exp.*	MCNP	Exp.	MCNP	Exp.	MCNP	Exp.	MCNP	Exp.	MCNP	Exp.
0.356	0.6341	0.6607	0.6627	0.6926	0.7183	0.7418	0.7666	0.7898	0.8138	0.8452	0.8795	0.9052
0.662	1.5175	1.5701	1.5620	1.6276	1.6812	1.7370	1.7742	1.8283	1.8594	1.9150	1.9739	2.0106
1.173	2.5954	2.6386	2.6726	2.7217	2.8426	2.8902	2.9668	3.0317	3.0734	3.1462	3.2277	3.3044
1.332	2.8167	2.8780	2.9064	2.9647	3.0973	3.1538	3.2389	3.2982	3.3503	3.4307	3.5195	3.6109

\*Exp. – experiment

**Table 5. The MCNP and available experimentally derived values of HVL for the six glass samples at gamma energy range (0.356-1.332) MeV**

Energy [MeV]	HVL [cm]											
	Sample 1		Sample 2		Sample 3		Sample 4		Sample 5		Sample 6	
	MCNP	Exp.*	MCNP	Exp.	MCNP	Exp.	MCNP	Exp.	MCNP	Exp.	MCNP	Exp.
0.356	0.4395	0.4580	0.4594	0.4799	0.4979	0.5141	0.5314	0.5473	0.5641	0.5857	0.6096	0.6273
0.662	1.0519	1.0881	1.0827	1.1279	1.1653	1.2040	1.2298	1.2670	1.2889	1.3271	1.3682	1.3933
1.173	1.7990	1.8285	1.8555	1.8861	1.9801	2.0029	2.0735	2.1010	2.1553	2.1803	2.2711	2.2899
1.332	1.9524	1.9945	2.0146	2.0545	2.1469	2.1856	2.2450	2.2857	2.3391	2.3775	2.4663	2.5024

\*Exp. – experiment

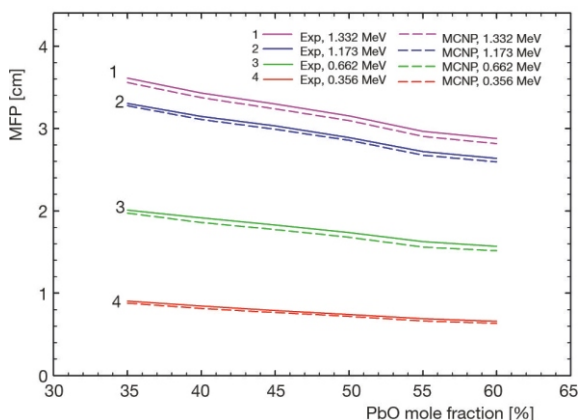


**Figure 3. Variation of MCNP and measured [15] MFP values with PbO concentration at gamma energy range 0.356-1.332 MeV**

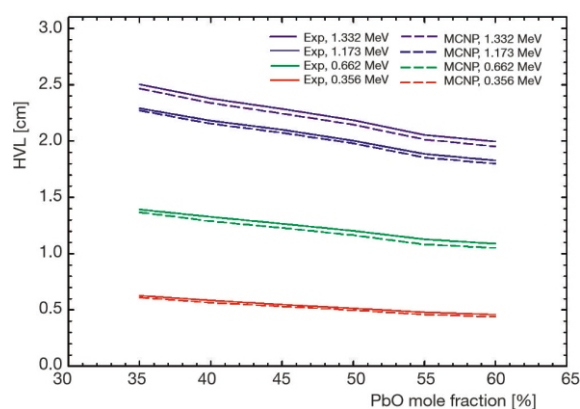


**Figure 4. Variation of MCNP and experimentally derived values of HVL with PbO concentration at gamma energy range 0.356-1.332 MeV**

## CONCLUSIONS

In this work, MCNP5 was used to develop a simple gamma transmission model and investigate its applicability in calculating  $\mu/\rho$ , MFP, and HVL values for the six simulated glass samples previously prepared by Kumar [15] and used for an experimental study. The MCNP values of  $\mu/\rho$ , MFP, and HVL shielding parameters were determined at twenty gamma energy lines ranging from 0.107 to 7.12 MeV and compared with those of XCOM and the available experimental values. In addition, the effect of PbO concentration on the simulated values of  $\mu/\rho$ , MFP, and HVL was also investigated and compared with the available experimental results at gamma energy lines of 0.356, 0.662, 1.1732, and 1.332 MeV.

It is found that the MCNP results follow a similar trend to the experimental results in [15] and therefore confirm the feasibility of using the currently proposed MCNP model to calculate photon attenuation parameters for different glass compositions, which is particularly useful in cases where no experimental data exist. On the other hand, the results demonstrate the applicability of the six glass samples as transparent shielding windows in nuclear reactors and isotope centers.

## ACKNOWLEDGEMENT

The author is grateful to the Department of Physics, College of Science, Al-Baha University for providing all the necessary facilities. The author thanks Ms. Antonietta Donzella of the University of Brescia for valuable discussions on the properties of MCNP.

## REFERENCES

- [1] Kaur, S., Singh, K. J., Investigation of Lead Borate Glasses Doped with Aluminium Oxide as gamma-ray Shielding Materials, *Annals of Nuclear Energy*, 63 (2014), Jan., pp. 350-354
- [2] Kurudirek, M., Heavy Metal Borate Glasses: Potential Use for Radiation Shielding, *Journal of Alloys and Compounds*, 727 (2017), Dec., pp. 1227-1236
- [3] Singh, V. P., Badiger, N. M., Shielding Efficiency of Lead Borate and Nickel Borate Glasses for gamma-rays and Neutrons, *Glass Physics and Chemistry*, 41 (2015), 3, pp. 276-283
- [4] El-Khayatt, A. M., et al., Photon Attenuation Coefficients of Heavy-Metal Oxide Glasses by MCNP Code, XCOM Program and Experimental Data: A Comparison Study, *Nuclear Instruments and Methods in Physics Research A*, 735 (2014), Jan., pp. 207-212
- [5] Medhat, M. E., Application of Gamma-Ray Transmission Method for Study the Properties of Cultivated Soil, *Annals of Nuclear Energy*, 40 (2012), 1, pp. 53-59
- [6] Turgut, U., et al., X-Ray Attenuation Coefficients Measurements for Photon Energies 4.508-13.375 keV in Cu, Cr and Their Compounds and the Validity of Mixture Rule, *Anal. Chim. Acta*, 515 (2004), 2, pp. 349-352
- [7] Akkurt, I., et al., Gamma-Ray Shielding Properties of Concrete Including Barite at Different Energies, *Prog. Nucl. Energy*, 52 (2010), 7, pp. 620-623
- [8] El-Khayatt, A. M., Radiation Shielding of Concrete Containing Different Lime/ Silica Ratios, *Ann. Nucl. Energy*, 37 (2010), 7, pp. 991-995
- [9] Lee, C. M., et al., Cracking Effect on Gamma-Ray Shielding Performance in Concrete Structure, *Prog. Nucl. Energy*, 49 (2007), 4, pp. 303-312
- [10] Chanthima, N., Kaewkhao, J., Investigation on Radiation Shielding Parameters of Bismuth Borosilicate Glass from 1 keV to 100 GeV, *Ann. Nucl. Energy*, 55 (2013), May, pp. 23-28
- [11] Kaundal, R. S., et al., Investigation of Structural Properties of Lead Strontium Borate Glasses for Gamma-Ray Shielding Applications, *J. Phys. Chem. Solids*, 71 (2010), 9, pp. 1191-1195
- [12] Kaewkhao, J., Limsuwan, P., Mass Attenuation Coefficients and Effective Atomic Numbers in Phosphate Glass Containing Bi<sub>2</sub>O<sub>3</sub>, PbO and BaO at 662 keV, *Nucl. Instrum. Meth. Phys. Res. A*, 619 (2010), 1-3, pp. 295-297
- [13] Kirdsiri, K., et al., Gamma-Rays Shielding Properties of xPbO:(100-x)B<sub>2</sub>O<sub>3</sub> Glasses System at 662 keV, *Ann. Nucl. Energy*, 36 (2009), 9, pp. 1360-1365
- [14] Singh, S., et al., Barium-Borate-Flyash Glasses: As Radiation Shielding Materials, *Nucl. Instrum. Meth. Phys. Res. B*, 266 (2008), 1, pp. 140-146
- [15] Kumar, A., gamma-ray Shielding Properties of PbO-Li<sub>2</sub>O-B<sub>2</sub>O<sub>3</sub> Glasses, *Radiation Physics and Chemistry*, 136 (2017), July, pp. 50-53
- [16] Tarim, U. A., Gurler, O., Source-To-Detector Distance Dependence of Efficiency and Energy Resolution of a 3" 3" NaI(Tl) Detector, *European Journal of Science and Technology*, (2018), 13, pp. 103-107
- [17] \*\*\*, X-5 Monte Carlo Team, MCNP-A General Monte Carlo N-Particle Transport Code: Overview and Theory, Los Alamos National Laboratory, Version 5, 2003
- [18] Elsheikh, N. A. A., Gamma-Ray and Neutron Shielding Features for Some Fast Neutron Moderators of interest in <sup>252</sup>Cf-Based Boron Neutron Capture Therapy, *Applied Radiation and Isotopes*, 156 (2020), Feb., p. 109012
- [19] Sharifi, S. H., et al., Comparison of Shielding Properties for Ordinary, Barite, Serpentine and Steel-Magnetite Concretes Using MCNP-4C Code and Available Experimental Results, *Ann. Nucl. Energy*, 53 (2013), Mar., pp. 529-534
- [20] El-Khayatt, A. M., Akkurt, I., Photon Interaction, Energy Absorption and Neutron Removal Cross Section of Concrete Including Marble, *Ann. Nucl. Energy*, 60 (2013), Oct., pp. 8-14
- [21] Tarim, U., et al., Monte Carlo Calculations for Gamma-Ray Mass Attenuation Coefficients of Some Soil Samples, *Annals of Nuclear Energy*, 58 (2013), Aug., pp. 198-201
- [22] Berger, M. J., et al., XCOM: Photon Cross Sections Database, NIST Standard Reference Database (XGAM), Available at: <http://www.nist.gov/pml/data/xcom/index.cfm>, 2010
- [23] Singh, K. J., et al., Gamma-Ray Shielding and Structural Properties of PbO-SiO<sub>2</sub> Glasses, *Nucl. Instr. Meth. Phys. Res. B*, 266 (2008), 6, pp. 944-948
- [24] Akman, F., et al., Comprehensive Study on Evaluation of Shielding Parameters of Selected Soils by Gamma and X-Rays Transmission in the Range 13.94-88.04 keV Using WinXCom and FFAST Programs, *Results in Physics*, 15 (2019), Dec., 102751
- [25] Akkurt, I., et al., Detection Efficiency of NaI(Tl) Detector in 511-1332 keV Energy Range, *Science and Technology of Nuclear Installations*, (2014), Article ID 186798
- [26] Demir, N., Kuluozturk, Z. N., Determination of Energy Resolution for a NaI(Tl) Detector Modeled with FLUKA Code, *Nuclear Engineering and Technology*, 53 (2021), 11, pp. 3759-3763
- [27] Alsayed, Z., et al., Study of some  $\gamma$ -Ray Attenuation Parameters for New Shielding Materials Composed of Nano ZnO Blended with High Density Polyethylene, *Nucl Technol Radiat*, 34 (2019), 4, pp. 342-352
- [28] Anh, N. T. K., et al., A Mathematical Function for Describing the Dependence of the Mass Attenuation Coefficient Versus Energy for Composite Materials in an Energy Range of 100 keV to 2 MeV, *Nucl Technol Radiat*, 34 (2019), 1, pp. 47-56
- [29] Sayyed, M. I., et al., An Extensive Investigation on gamma-ray Shielding Features of Pd/Ag-Based Alloys, *Nuclear Engineering and Technology*, 51 (2019), 3, pp. 853-859
- [30] Huq, M. F., et al., Calculation of Gamma-Ray Attenuation Parameters for Locally Developed Shielding Material: Polyboron, *Journal of Radiation Research and Applied Sciences*, 9 (2016), 1, pp. 26-34

Received on August 12, 2021

Accepted on January 26, 2022

**Насреддин А. А. ЕЛШЕИК**

**МОНТЕ КАРЛО МОДЕЛ ТРАНСМИСИЈЕ ГАМА  
ЗРАЧЕЊА ЗА КАРАКТЕРИЗАЦИЈУ МУЛТИ-ГАМА ЗАШТИТНОГ  
СТАКЛА ОД ОКСИДА ТЕШКИХ МЕТАЛА**

Применљивост једноставног Монте Карло гама трансмисионог модела испитана је карактеризацијом масеног коефицијента слабљења, средњег слободног пута и полудебљине за шест симулираних узорака од стакла састава  $PbO-Li_2O-B_2O_3$ , које су претходно други припремили. Израчунати су масени коефицијенти слабљења и упоређени са онима добијеним ХСОМ програмом и доступним експерименталним подацима за двадесет гама енергетских линија од 0,107 MeV до 7,12 MeV, са добрим слагањем. Ефекти PbO концентрације на симулиране вредности масеног коефицијента слабљења, средњег слободног пута и полудебљине слоја, израчунати су и упоређени са доступним експерименталним подацима у опсегу енергије гама зрачења од 0,356 MeV до 1,332 MeV, и такође је утврђена добра сагласност. Узорак стакла са оптималном гама заштитом за све разматране гама енергије био је узорак са хемијском формулом  $Pb_3B_4O_9$ . Са једне стране, резултати MCNP програма потврђују применљивост предложеног модела за извођење додатних прорачуна својстава слабљења фотона за различите саставе стакла, а са друге стране, с обзиром на енергетски опсег фотона гама зрачења у реактору током фисије уранијума од 0,10 MeV до 10 MeV, резултати сугеришу да се испитивани узорци стакла користе као оптички заштитни прозори у нуклеарним реакторима.

*Кључне речи: Монте Карло симулација, ХСОМ, стакло од оксида тешких метала,  
параметар заштите од гама зрачења*

---